

# Hardware Accelerator and Neural Network Co-Optimization for Ultra-Low-Power Audio Processing Devices

Gerum Christoph\*

Department of Computer Science  
University of Tübingen  
christoph.gerum@uni-tuebingen.de

Frischknecht Adrian\*

Department of Computer Science  
University of Tübingen  
adrian.frischknecht@uni-tuebingen.de

Hald Tobias

Department of Computer Science  
University of Tübingen  
tobias.hald@student.uni-tuebingen.de

Palomero Bernardo Paul

Department of Computer Science  
University of Tübingen  
paul.palomero-bernardo@uni-tuebingen.de

Lübeck Konstantin

Department of Computer Science  
University of Tübingen  
konstantin.luebeck@uni-tuebingen.de

Bringmann Oliver

Department of Computer Science  
University of Tübingen  
oliver.bringmann@uni-tuebingen.de

**Abstract**—The increasing spread of artificial neural networks does not stop at ultralow-power edge devices. However, these very often have high computational demand and require specialized hardware accelerators to ensure the design meets power and performance constraints. The manual optimization of neural networks along with the corresponding hardware accelerators can be very challenging. This paper presents HANNAH (Hardware Accelerator and Neural Network seArch), a framework for automated and combined hardware/software co-design of deep neural networks and hardware accelerators for resource and power-constrained edge devices. The optimization approach uses an evolution-based search algorithm, a neural network template technique and analytical KPI models for the configurable UltraTrail hardware accelerator template in order to find an optimized neural network and accelerator configuration. We demonstrate that HANNAH can find suitable neural networks with minimized power consumption and high accuracy for different audio classification tasks such as single-class wake word detection, multi-class keyword detection and voice activity detection, which are superior to the related work.

**Index Terms**—Machine Learning, Neural Networks, AutoML, Neural Architecture Search

## I. INTRODUCTION

Artificial intelligence is increasingly spreading into the domain of always-on ultra-low power connected devices like fitness trackers, smart IoT sensors, hearing aids and smart speakers. The limited power budget on these devices and the high computational demand often mandates the use of specialized ultra-low power hardware accelerators, specialized to a specific application or application domain. Hardware design, neural network training and optimized deployment often require manual optimization by the system designers, who need to deal with manifold often counter-directed issues. In this

This work has been partly funded by the EU and the German Federal Ministry of Education and Research (BMBF) in the projects OCEAN12 (reference number: 16ESE0270).

\*These authors contributed equally to this work.

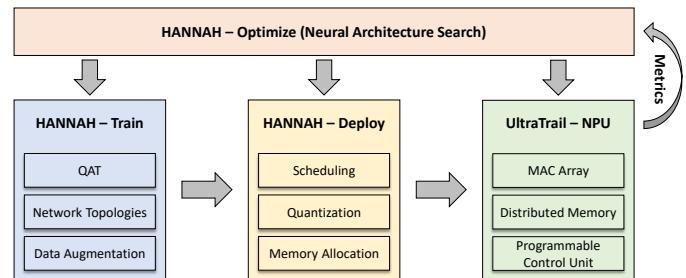


Fig. 1: Overview of the HANNAH framework.

work, we propose HANNAH (Hardware Accelerator and Neural Network seArch) to automatically co-optimize neural network architectures and a corresponding neural network accelerator.

The HANNAH design flow is shown in Figure 1. Neural Networks are instantiated and trained in the training component employing quantization aware training and dataset augmentation. Trained neural networks are then handed over to the deployment component (Sec. III) for target code generation. Here, the neural network is quantized to a low word width representation the neural network operations are scheduled and on-device memory is allocated for the neural network. Along with the target network architecture, a specialized hardware accelerator for the neural network processing is instantiated from a configurable Verilog template. Hardware dependent performance metrics like power consumption and chip area are then either generated by running the neural network on a gate-level simulation or estimated using an analytical performance model. The evolution-based search strategy (Sec. IV) implemented in the HANNAH optimizer is then used to incrementally search the neural network and hardware accelerator codesign space.

The main contributions of this paper are:

- 1) We present an end-to-end design flow from neural network descriptions down to synthesis and gate-level



**Algorithm 1:** Pseudocode of the NPU accelerator when configured with an  $N \times N$ -MAC array with  $K$  output channels,  $C$  input channels,  $F$  filter size,  $S$  stride,  $I$  input length,  $X = \lfloor (I-1)/S \rfloor + 1$  output length, and full padding.

```

1 for k = 0 :  $\lceil K/N \rceil$  do
2   for c = 0 :  $\lceil C/N \rceil$  do
3     for f = 0 : F do
4       for x = 0 : X do
5          $i_{idx} \leftarrow x \cdot S - \lfloor F/2 \rfloor + f$ 
6         if  $i_{idx} \geq 0$  and  $i_{idx} < I$  then
7            $1^{(N)}[x] += i^{(N)}[c][i_{idx}] \cdot w^{(N \times N)}[k][c][f]$ 
8       for x = 0 : X do
9          $o^{(N)}[k][x] = \text{opu}(1^{(N)}[x])$ 

```

The backend extracts weights and biases from the model. These parameters are padded and reordered to fit the expected data layout before they get quantized to the defined fixed-point format. The same happens to example input data provided by HANNAH which is used as simulation input.

The word widths of the internal LMEM memory are calculated by the largest fixed-point format times two plus the logarithm of the maximum input channels to avoid an overflow.

After the schedule and number of weights and biases are fixed, the deployment backend generates the corresponding 22FDX memory macros. The backend determines the size and word width of the weight and bias memory from the fixed numbers. The schedule gets analyzed to determine the size of each FMEM so that the feature maps fit perfectly for the trained neural network. All memory sizes can be adjusted manually to support other neural networks with more parameters or larger feature maps. The LMEM size is determined by the largest supported output feature map. All memory sizes and word widths are set to the next possible memory macro configuration.

Given the generated configuration, weights and biases, memory macros, example input data, and selected hardware parameters, a simulation, synthesis, and power estimation are run automatically if desired. The simulation results are fed back to HANNAH and compared with the reference output to validate the functional correctness of the accelerator.

### C. NPU Models

The simulation and synthesis of UltraTrail are time-consuming and therefore not feasible for hundreds to thousands of possible configurations. To get an accurate yet fast evaluation of UltraTrail, performance, area, and power consumption are estimated using analytical models.

For latency estimation we adopt the cycle-accurate analytical model presented in [12] to configurable array sizes. The pseudocode shown in Algorithm 1 visualizes the NPU operations and memory accesses. The accelerator iterates over  $C$  input and  $K$  output channels tiled by the MAC array size

$N$ . One  $N \times N$  patch of the weight array is fetched from the weight memory per iteration of the next loop. In the innermost loop  $N$  input channels are fetched from one of the FMEMs and the current convolution outputs are accumulated in the LMEM using a spatially unrolled matrix-vector multiplication on the MAC array. To avoid misaligned memory accesses and accelerate the computation, padding is implemented by skipping the corresponding loop iterations instead of actual zero padding of the feature maps. In the last loop, the OPU fetches  $N$  output channels from the LMEM and the  $N$  results are stored in a planned FMEM. The latency of the accelerator without skipping of padded values can be easily estimated using the following equation, by just counting the number of loop iterations.

$$l = 1 + \left\lceil \frac{C}{N} \right\rceil \cdot \left\lceil \frac{K}{N} \right\rceil \cdot F \cdot X \quad (1)$$

Where the output length  $X$  can be derived from input length  $I$  using  $X = \lfloor (I-1)/S \rfloor + 1$ . The crucial part of the performance model is to accurately calculate the number of skipped loops in Line 7 of Algorithm 1. For the case  $i_{idx} \geq 0$  skipping happens in the first  $a_{p,b} = \left\lfloor \frac{\lfloor F/2 \rfloor - 1}{S} + 1 \right\rfloor$  iterations over  $x$ , the number of skipped executions is  $\lceil \frac{F}{2} \rceil$  at the start of the loop, and decreases by  $S \cdot i$  for each iteration over  $X$ . For the case  $i_{idx} < I$  the analytical model is similar but special care must be taken if the input length  $I$  is not divisible by the stride. In the last iteration over  $x$ ,  $i_{idx}$  takes the value  $I_{max} = (X-1) \cdot S - \lfloor F/2 \rfloor + F - 1$  leading to an effective padding of  $C_{w,e} = I_{max} + 1 - \lfloor F/2 \rfloor - I$ . Loop skipping then happens for the last  $a_{p,e} = \left\lfloor \frac{\lfloor C_{w,e} \rfloor - 1}{S} + 1 \right\rfloor$  iterations. The number of skipped iterations is  $C_{w,e}$  at the end of the loop and also decreases by  $s \cdot i$  at each loop iteration. This leads to an estimation of the total number of skipped MAC array operations at the beginning  $\#MAC_{not,b}$  and end  $\#MAC_{not,e}$  of the loop as:

$$\#MAC_{not,b} = \sum_{i=0}^{a_{p,b}-1} \left\lfloor \frac{F}{2} \right\rfloor - s \cdot i \quad (2)$$

$$\#MAC_{not,e} = \sum_{i=0}^{a_{p,e}-1} \lfloor C_{w,e} \rfloor - s \cdot i \quad (3)$$

And a total per layer latency of:

$$l = 1 + \left\lceil \frac{C}{N} \right\rceil \cdot \left\lceil \frac{K}{N} \right\rceil \cdot F \cdot X - \#MAC_{not,e} - \#MAC_{not,b} \quad (4)$$

The power model has two parts for SRAM power estimation and for other NPU components. For every layer and memory, the model calculates the number of read, write, and nop (idle) operations. LMEM and input feature memory (IMEM) are accessed at each cycle of the operation except for a single setup cycle. The read cycles  $r_{imem}$  and  $r_{lmem}$  and write cycles  $w_{lmem}$  are the same as the layer latency  $l-1$ . As the number of memory accesses to the weights remain stationary during the

innermost loop of Algorithm 1, the weight memory is accessed only  $\lceil \frac{C}{N} \rceil \cdot \lceil \frac{K}{N} \rceil \cdot F$  times ( $r_{wmem}$ ). Memory access to the output feature memory ( $w_{omem}$ ), the bias memory ( $r_{bmem}$ ), and in the case of residual blocks the partial sum feature memory ( $r_{pmem}$ ) is given as  $\lceil K/N \rceil \cdot X$ . Idle times for the memories are then calculated using the layer latencies and access times for each memory:  $i_m = l - r_m - w_m$

Furthermore, the combinational MAC array alone causes many relevant glitches related to SRAM. Therefore, the glitching LMEM data input leads to a non-negligible power increase. Based on some gate-level simulations for different networks and array sizes, a linear regression for the number of glitches ( $gl_{mem}$ ) is used.

Finally, if the network latency on the accelerator  $L$  is below the period  $P$  for real time operation, the memories are switched to low power modes with reduced leakage for the remainder of the period. The final power consumption of the memories is then estimated using:

$$P_{mem} = \frac{L}{P} \cdot P_{lmem}^{(glitch)} \cdot gl_{mem} + \sum_m \frac{L}{P} (P_m^{(read)} \cdot r_m + P_m^{(write)} \cdot w_m + P_m^{(idle)} \cdot i_m) + \frac{L}{P} \cdot P_m^{(static)} + \left(1 - \frac{L}{P}\right) \cdot P_m^{(lp)} \quad (5)$$

The dynamic power  $P_m^{(read)}$ ,  $P_m^{(write)}$ ,  $P_m^{(idle)}$ ,  $P_{lmem}^{(glitch)}$  and static power in running-  $P^{(static)}$  and low power-mode  $P^{(lp)}$  are extracted from the memory compiler for each memory macro usable during the co-optimization and stored in a database.

Again, the model assumes a constant value for the control unit as the power consumption is mainly independent of the configuration and executed neural network. The power consumption of the MAC array and OPU is approximated using a linear regression on MAC array size and word width of the MAC array calibrated using gate-level simulations. Note, that the dynamic power for non-memory modules is weighted depending on the runtime per inference.

The analytical area model comprises an exact SRAM area calculation and an estimation for the other NPU components to estimate the cell area of the NPU after synthesis. The model looks up the SRAM area in a small database containing all necessary memory macros used during NAS. The SRAM area estimation is by far the most important as it is responsible for about 90% of the total synthesis cell area. The control unit is mainly independent of the configuration and its area is modelled as constant. The MAC array is estimated by a linear growth of the word width and quadratic growth of the MAC array dimension based on a minimum MAC unit area. The OPU model is like the MAC array model however grows linear with MAC array size.

#### IV. NEURAL NETWORK / HARDWARE CO-OPTIMIZATION

The co-optimization uses a block based search space for neural network architectures. As shown in Figure 3a each

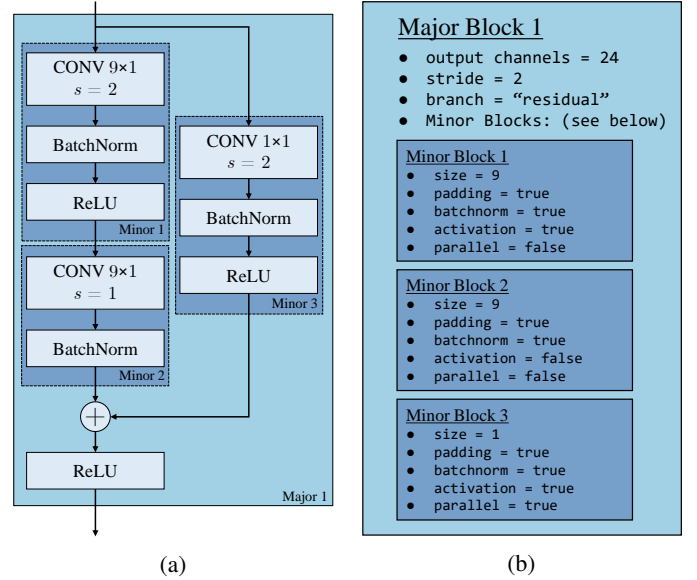


Fig. 3: A subgraph of the search space build from blocks and layers (a) and the corresponding abstract configuration (b).

TABLE I: Neural Architecture Search Space

Level	Option	Choices
Network	Word Width Features	4,6,8
Network	Word Width Weights	2,4,6,8
Network	Number of Blocks	1-4
Block	Stride of Blocks	1,2,4,8,16
Block	Type	residual, forward
Block	Number of Convs	1-4
Layer	Kernel Size	1,3,5,7,9,11
Layer	Output Channels	4,8,...,64
Layer	Activation Function	ReLU, None
Accelerator	Array Size	2 × 2, 4 × 4, 8 × 8, 16 × 16
Accelerator	Memory Sizes	imputed
Accelerator	Word Widths	imputed

block is either a residual block with a main branch of a configurable number of convolutional layers on the trunk and a skip connection or a simple feed forward CNN block leaving out the skip connection. We additionally search over layer, block and network level hyperparameters like filter size, stride and convolution sizes. The hardware accelerator search space consists of the MAC array dimensions, the memory sizes and multiplier word widths. The mac array size is optimized using the search algorithm while the other metrics are derived from the neural network parameters, during neural network deployment. A full overview of the parameters is shown in Table I.

The search for a target neural network and accelerator architecture configuration is implemented as an evolution-based multi-objective optimization. As shown in Algorithm 2, the search first samples random neural network and hardware configuration from a joint search space  $S$ . The neural network is then trained using quantization aware training, and the trained neural network is then evaluated on the validation set to obtain the accuracy metric. All further performance metrics are estimated by the analytical hardware model as described in Section III. At the end of an optimization step, the

sampled architecture parameters and the performance metrics are added to the search history. After the initial population size  $s$  has been reached, new architectures are derived from the current population using element-wise mutations. During search, HANNAH randomly samples from the following set of mutations:

- 1) Add/remove a block
- 2) Change block type between residual and feed-forward
- 3) Add/remove a convolutional layer
- 4) Increase/decrease convolution size
- 5) Increase/decrease major block stride
- 6) Increase/decrease quantization word width
- 7) Increase/decrease MAC array size
- 8) Increase/decrease number of output channels

To select the ancestor of the next evaluation point. Similar to current neural network search for TinyML on microcontrollers [8], [9], we adopt randomized scalarization [21].

In this approach the architecture parameters are ranked according to the following scalarization function:

$$f(M) = \max_{m_i \in M} \lambda_i \cdot m_i \quad (6)$$

The  $\lambda_i$  are sampled from the uniform distribution over  $[0, \frac{1}{b_i}]$  where  $b_i$  denotes a soft boundary for each target metric. Choosing  $\lambda_i$  in this way ensures that candidates violating soft targets are always ranked behind targets that satisfy a target, while on the other hand encouraging the search to explore different parts of the search space near the Pareto boundary.

## V. EXPERIMENTAL EVALUATION

The HANNAH framework has been implemented using current best practice libraries, using PyTorch version 1.10.1 [22].

Training hyperparameters have been set to fixed values for all experiments. All training runs use 30 epochs and use a batch size of 128 samples per minibatch. The optimizer used for training the network parameters is adamW with a one-cycle learning rate scheduling policy using a maximum learning rate of 0.005. All other optimizer and learning rate parameters are left at the default values provided by PyTorch. All searches are run on a machine learning cluster using 4 Nvidia RTX2080 Ti GPUs. We train 8 neural network candidates in parallel which takes approximately 10 minutes. The training uses noisy quantization aware training [23]. The training sets are augmented using the provided background noise files for keyword spotting and voice activity detection and using random white noise for wake word detection. For inference the batch norm weights are folded into the weights and bias of the preceding convolutional layer [24].

As the hardware accelerator is set to operate at 250 kHz and the neural networks are trained and evaluated with an input time shift of 100 ms we set the latency constraint of the neural network architectures to 25.000 cycles corresponding to the maximum input shift used during training and evaluation. The area constraints are set to  $150\,000\ \mu\text{m}^2$  which is slightly less than the configuration used in [12] for KWS. The constraints for

---

### Algorithm 2: Neural architecture and Hardware Accelerator Search

---

**Input:** Design Space  $S$ , Search Budget  $b$ , Population Size  $s$ , Bounds  $B$ , Training Set  $T$ , Validation Set  $V$

**Output:** Search History  $H$

```

/* Start with empty search history */
1  $H \leftarrow \emptyset$ 
2 for  $n \in \{1 \dots b\}$  do
3   if  $b \leq s$  then
4     /* Sample Random Architecture and Accelerator */
5      $a \leftarrow \text{sample\_random}(S)$ 
6   else
7     /* Sample Fitness Function from target bounds */
8      $f \leftarrow \text{sample\_fitness\_function}(B)$ 
9     /* Sort last  $p$  candidates according to Fitness */
10     $P \leftarrow \text{sort}(H[-s:], f)$ 
11    /* Apply random mutation to current best architecture */
12     $a \leftarrow \text{mutate\_random}(\text{last}(P))$ 
13  /* Quantization Aware Training */
14   $N \leftarrow \text{train}(a, T)$ 
15  /* Evaluate trained architecture */
16   $\text{error\_rate} \leftarrow \text{evaluate}(N, V)$ 
17  /* Estimate other metrics from hardware model */
18   $\text{power, latency, area} \leftarrow \text{hardware\_model}(a)$ 
19  /* Append architecture and metrics to history */
20   $H.\text{append}(a, (\text{error\_rate}, \text{power}, \text{latency}, \text{area}))$ 

```

---

KWS are set to  $5\ \mu\text{W}$  maximum power and accuracy constraints are set to 93.0%. The other tasks use a power budget of  $1\ \mu\text{W}$  and accuracy constraints of 95.0%. All searches ran with a search budget of 3000 individual architectures and use a population size of 100.

We use the 22FDX technology by GlobalFoundries for implementation with low-leakage standard cells and SRAMs from Invecas. For synthesis and power estimation we use Cadence Genus 20.10 and Cadence Joules 21.11, respectively. For the average power consumption, we use two separate power estimations for the inference with previous feature loading and idle time. A weighted sum adds these two parts accordingly. The load of weights and bias is not included as it must be performed only once. It is evaluated at a  $25\ ^\circ\text{C}$  TT corner with 0.8 V supply voltage and no body bias voltage. The NPU uses clock-gating and low-power modes of the SRAM during idle times and waiting for the next inference to start.

#### A. Results of Neural Network Co-Optimization

Figure 4 shows a summary of the NAS results. For the three evaluation datasets, the search focuses the evaluated



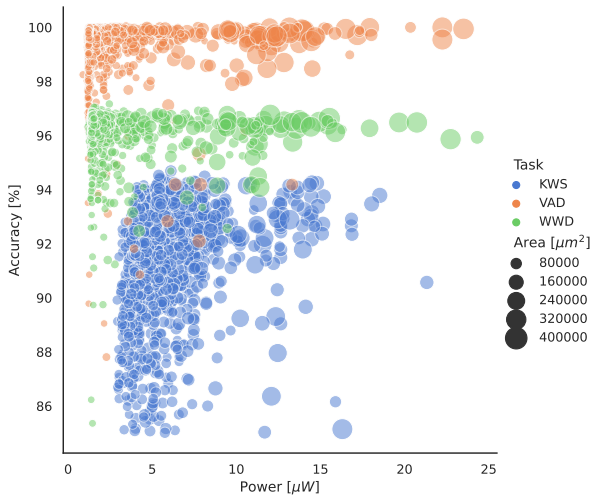


Fig. 4: Summarized power, area, and accuracy results

architectures around the Pareto front of power and accuracy, and is able to find good trade-offs of power and accuracy. For further analysis we select the Pareto points with lowest power (LP) and highest accuracy (HA) which are shown in Figure 5. Half of the chosen networks are simple feed-forward convolutional neural networks, while the other half of neural networks contain at least one residual block. The chosen networks sizes and operator configurations reflect the difficulty of the different machine learning tasks. The harder tasks use deeper networks, fewer strides and generally smaller convolution kernels, while the easier tasks use very shallow networks with rather bit convolution kernels. These bigger filters are needed to compensate for the extremely big strides used in the operator configurations. In all of the networks the search algorithm identified, possibilities to introduce bottlenecks, e.g. convolutions with a larger number of output channels followed convolutions with comparably fewer output channels.

### B. NPU Models

Figure 6 shows the deviation in percentage points of the predictions of the analytical models and the data obtained from RTL simulation, synthesis and gate-level power estimation for latency, cell area and power consumption, respectively.

The analytical performance model has no deviation as the behavior of the hardware accelerator is modelled exactly.

The area model slightly underestimates by 2.41-4.06 percentage points because only the memory macros are exactly modelled and the other components do not handle quadratic growth. The deviation to the total synthesis area is additionally about 3.6%.

The power model uses the performance model to calculate the inference and idle time. Regarding the gate-level power consumption the power model results are in the range of  $-9.19$ – $-0.2$  percent points. Like the area model, the power model does not handle any non-linearity despite the array size. In addition, the chosen minimum value for the MAC array and OPU is conservative and has higher deviations for larger configurations like the ones for KWS. Also, the model does

not consider any data dependent or parasitic induced power consumption. The NPU models are valid to guide the neural network co-optimization regarding performance and area with high precision.

### C. Comparison to related work

Note, that due to the differences in datasets, technology, and the components contained in the system, a direct comparison is only possible to a limited extent. All our implementations have a positive slack that allows at least a clock frequency of 13.3 MHz without changing the voltage nor the synthesized netlist. This allows to reduce the latency but the power consumption would increase linearly with the clock frequency. For our work, the tables list the latency for feature loading and subsequent inference, as well as the latency with applied power gating. The corresponding power consumptions are also listed.

1) *Keyword Spotting*: Table II lists state-of-the-art KWS accelerators and systems. [13] uses a recurrent neural network with LSTM units to detect only four keywords and has a higher power consumption than both of our variants. [14] proposes a system with feature extraction and a hierarchical accelerator setup including a sound detector, a KWS and a speaker validation module to reduce power consumption. The system in [15] also includes a feature extraction but nevertheless with  $41.3 \mu\text{W}$  has a higher power consumption than all other works. Our LP and HA variants are based on [12] and achieve the highest accuracy on GSCD while both variants still have a lower power consumption.

2) *Voice Activity Detection*: State-of-the-art VAD accelerators and systems are shown in Table III. Note that almost all chosen datasets, technologies and latencies are different. Price et al. [16] uses a VAD accelerator for a fully connected neural network as a preliminary stage with a power consumption of  $22.3 \mu\text{W}$  and a latency of at least 100 ms. [19] presents an ultra-low power VAD accelerator for binary neural networks. The power consumption varies between 2 and  $8 \mu\text{W}$  depending on the used word width with speech accuracy of up to 95% with 10 dB of restaurant noise. [20] uses an analogue front end (AFE) to calculate the features and so the overall system consumes just about  $1 \mu\text{W}$ . The accelerator itself has a low latency and power consumption but also a low accuracy compared to other works. Our variants have the lowest power consumption and highest accuracies without noise and a latency of 100 ms.

3) *Wake Word Detection*: State-of-the-art WWD accelerators and systems are shown in Table IV using the “Hey Snips” dataset. [17] uses spiking neural networks combined with event-driven clock and power gating to reduce the power consumption. This is the only state of the art accelerator that can beat our work in some of the accuracy and power values, but needs a very specialized neural network and hardware accelerator architecture. [18] proposes a system with accelerators for feature extraction, VAD and binary RNNs. This system has a lower accuracy and higher power consumption than our accelerators.

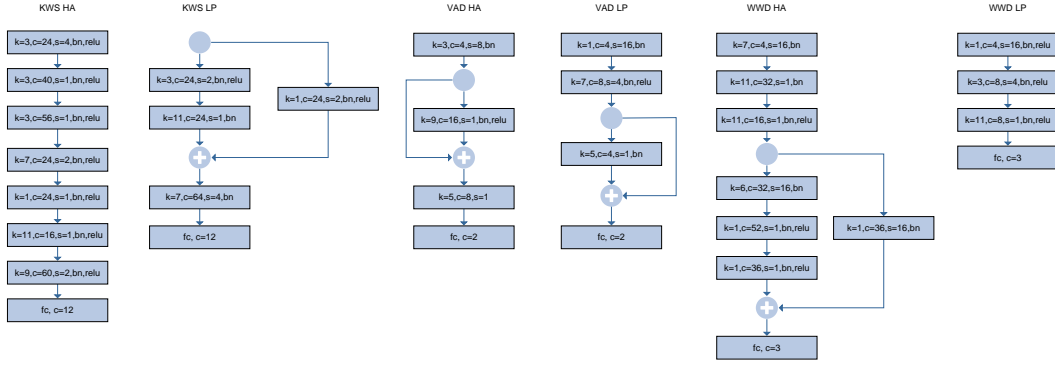


Fig. 5: Low power and high accuracy network configurations for the three search tasks (fc = fully connected layer, bn = batch norm, relu = rectified linear unit, k=kernel size, c=number of output channels, s = stride)

TABLE II: Comparison of Results on Keyword Spotting Task

	ESSCIRC'2018 [13]	ISSCC'2020 [14]	IEEE Access [15]	ESWEEK'2020 [12]	High Accuracy	Low Power
Technology	65 nm	65 nm	22 nm	22 nm	22 nm	22 nm
Area	1.03 mm <sup>2</sup> <sup>c</sup>	2.56 mm <sup>2</sup> <sup>c</sup>	0.75 mm <sup>2</sup> <sup>c</sup>	0.20 mm <sup>2</sup> <sup>c</sup>	0.126 mm <sup>2</sup> <sup>d</sup>	0.118 mm <sup>2</sup> <sup>d</sup>
Frequency	250 kHz	250 kHz	250 kHz	250 kHz	250 kHz	250 kHz
Latency	16 ms	16 ms	20 ms	100 ms	100 ms	100 ms
Voltage	0.6 V	0.6 V	0.55 V	0.8 V	0.8 V	0.8 V
DNN Structure	LSTM+FC	LSTM+FC	CONV+FC	TC-ResNet	CONV+FC	TC-ResNet
Word Width (Weights)	4/8	4/8	7	6	6	6
Word Width (Inputs)	8	8	8	8	6	6
MAC Array Size	-	-	-	8 × 8	8 × 8	8 × 8
Accuracy <sup>a</sup>	-	90.87 % (GSCD)	90.51 % (GSCD)	93.09 % (GSCD)	94.73 % (GSCD)	93.54 % (GSCD)
F1-Score <sup>a</sup>	90.00 % (TIMIT) <sup>b</sup>	-	-	-	94.73 % (GSCD)	93.54 % (GSCD)
Keywords	4	10	10	10	10	10
Power	5.0 μW	10.6 μW	52 μW	8.2 μW	4.73 μW	4.17 μW
					10.4 μW <sup>f</sup>	10.7 μW <sup>f</sup>

<sup>a</sup> SNR ≥ 1000 dB

<sup>b</sup> Note the difference in datasets

<sup>c</sup> Area for layout/chip

<sup>d</sup> Cell area for synthesis

<sup>e</sup> Active inference latency

<sup>f</sup> Power when active

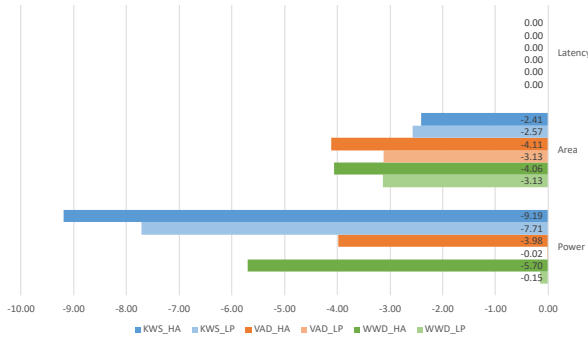


Fig. 6: Deviation of analytical models from gate-level simulation results in percentage points.

## VI. CONCLUSION AND FUTURE WORK

In this paper, we have presented HANNAH, a framework for co-optimization of neural networks and corresponding hardware accelerators. The framework is able to find neural networks to automatically find and generate ultra-low power implementations on a set of three speech processing benchmarks. In our future work we intend to extend this work to support

heterogeneous deployments and a larger class of DNNs for intelligent sensor processing and perception in edge devices.

## REFERENCES

- [1] H. Pham et al., “Efficient neural architecture search via parameters sharing,” in *International Conference on Machine Learning*. PMLR, 2018.
- [2] B. Zoph et al., “Learning transferable architectures for scalable image recognition,” in *IEEE conference on computer vision and pattern recognition*, 2018.
- [3] H. Liu et al., “Hierarchical representations for efficient architecture search,” *arXiv preprint arXiv:1711.00436*, 2017.
- [4] Y. Yang et al., “Synetgy: Algorithm-hardware co-design for convnet accelerators on embedded fpgas,” in *2019 International Symposium on Field-Programmable Gate Arrays*, 2019.
- [5] M. S. Abdelfattah et al., “Best of both worlds: Automl codesign of a cnn and its hardware accelerator,” in *57th ACM/IEEE Design Automation Conference*. IEEE, 2020.
- [6] W. Jiang et al., “Hardware/software co-exploration of neural architectures,” *IEEE Transactions on Computer-Aided Design of Integrated Circuits and Systems*, vol. 39, no. 12, pp. 4805–4815, 2020.
- [7] Y. Zhou et al., “Rethinking co-design of neural architectures and hardware accelerators,” *arXiv preprint arXiv:2102.08619*, 2021.
- [8] E. Liberis, Ł. Dudziak, and N. D. Lane, “ $\mu$ nas: Constrained neural architecture search for microcontrollers,” in *1st Workshop on Machine Learning and Systems*, 2021.

TABLE III: Comparison of Results on Voice Activity Detection Task

	ISSC'2017 [16]	JSSC'2019 [19]	GLSVLSI'2020 [20]	High Accuracy	Low Power
Technology	65 nm	28 nm	180 nm	22 nm	22 nm
Area	-	-	0.62 mm <sup>2</sup> (estimated NPU)	0.050 mm <sup>2</sup>	0.036 mm <sup>2</sup>
Frequency	1.68 MHz-47.8 MHz	-	-	250 kHz	250 kHz
Latency	100 ms-500 ms	10 ms	10 ms	100 ms	100 ms
Voltage	0.5 V-0.9 V	0.55 V	0.55 V	9.1 ms <sup>a</sup>	4.5 ms <sup>a</sup>
DNN Structure	FC	FC	FC	0.8 V	0.8 V
Word Width (Weights)	16 (from [19])	1	1	TC-ResNet	TC-ResNet
Word Width (Inputs)	16 (from [19])	1/4/8	9 (first layer), 1 (else)	4	2
MAC Array Size	-	-	-	4 × 4	4 × 4
Accuracy	10.0 % EER @7 dB (AURORA2)	95/92.0 % @10 dB 90/87.0 % @5 dB 85/80.0 % @-5 dB (TIMIT, Noise-92)	84/85 % @10 dB (Aurora4, DEMAND)	99.88 % 99.43 % @10 dB 99.40 % @5 dB 98.04 % @0 dB (UW/NU,TUT)	97.17 % 95.37 % @10 dB 93.04 % @5 dB 88.90 % @0 dB (UW/NU,TUT)
Power	22.3 μW	2/5/8 μW	1.01 μW@AFE+VAD 0.63 μW@VAD only	851 nW 4.17 μW <sup>b</sup>	435 nW 2.13 μW <sup>b</sup>

<sup>a</sup> Active inference latency<sup>b</sup> Power when active

TABLE IV: Comparison of Results on Wake Word Detection Task

	arXiv'2020 [17]	VLSI'2019 [18]	High Accuracy	Low Power
Technology	65 nm	65 nm	22 nm	22 nm
Area	1.99 mm <sup>2</sup>	6.2 mm <sup>2</sup> (FE+NPU)	0.046 mm <sup>2</sup>	0.036 mm <sup>2</sup>
Frequency	70 kHz	5-75 MHz	250 kHz	250 kHz
Latency	-	3.36 μs-1.91 ms	100 ms	100 ms
Voltage	0.5-1.0 V	0.9-1.1 V	18.2 ms <sup>a</sup>	5.4 ms <sup>a</sup>
DNN Structure	SNN	RNN	0.8 V	0.8 V
Word Width (Weights)	6	1	TC-ResNet	CONV+FC
Word Width (Inputs)	1	1	4	2
MAC Array Size	-	-	4 × 4	4 × 4
Accuracy	95.8 % @40 dB -90.5 % @0 dB	91.9 %	96.81 % 95.8 % @40 dB 94.6 % @0 dB	95.64 % 95.3 % @40 dB 95.1 % @0 dB
Power	75-220 nW	134 μW	998 nW 4.15 μW <sup>b</sup>	435 nW 2.14 μW <sup>b</sup>

<sup>a</sup> Active inference latency<sup>b</sup> Power when active

- [9] I. Fedorov et al., "Sparse: Sparse architecture search for cnns on resource-constrained microcontrollers," *Advances in Neural Information Processing Systems*, vol. 32, 2019.
- [10] J. Lin et al., "Mcunet: Tiny deep learning on iot devices," *arXiv preprint arXiv:2007.10319*, 2020.
- [11] C. Banbury et al., "Micronets: Neural network architectures for deploying tinyml applications on commodity microcontrollers," *Proceedings of Machine Learning and Systems*, vol. 3, 2021.
- [12] P. P. Bernardo et al., "Ultratrail: A configurable ultralow-power tc-resnet ai accelerator for efficient keyword spotting," *IEEE Transactions on Computer-Aided Design of Integrated Circuits and Systems*, vol. 39, no. 11, pp. 4240–4251, 2020.
- [13] J. S. Giraldo and M. Verhelst, "Laika: A 5uw programmable lstm accelerator for always-on keyword spotting in 65nm cmos," in *IEEE 44th European Solid State Circuits Conference*. IEEE, 2018, pp. 166–169.
- [14] J. S. P. Giraldo et al., "Vocell: A 65-nm Speech-Triggered Wake-Up SoC for 10-μW Keyword Spotting and Speaker Verification," *IEEE Journal of Solid-State Circuits*, 2020.
- [15] B. Liu et al., "An Ultra-Low Power Always-On Keyword Spotting Accelerator Using Quantized Convolutional Neural Network and Voltage-Domain Analog Switching Network-Based Approximate Computing," *IEEE Access*, vol. 7, pp. 186456–186469, 2019.
- [17] D. Wang et al., "Always-on, sub-300-nw, event-driven spiking neuromorphic network based on spike-driven clock-generation and clock-and power-gating for an ultra-low-power intelligent device," *arXiv preprint arXiv:2006.12314*, 2020.
- [18] R. Guo et al., "A 5.1 pj/neuron 127.3 us/inference rnn-based speech recognition processor using 16 computing-in-memory sram macros in 65nm cmos," in *2019 Symposium on VLSI Circuits*, 2019.
- [19] M. Yang et al., "Design of an always-on deep neural network-based 1-μw voice activity detector aided with a customized software model for analog feature extraction," *IEEE Journal of Solid-State Circuits*, vol. 54, no. 6, pp. 1764–1777, 2019.
- [20] B. Liu et al., "A background noise self-adaptive vad using snr prediction based precision dynamic reconfigurable approximate computing," in *2020 Great Lakes Symposium on VLSI*, 2020.
- [21] B. Paria, K. Kandasamy, and B. Póczos, "A flexible framework for multi-objective bayesian optimization using random scalarizations," in *Uncertainty in Artificial Intelligence*. PMLR, 2020.
- [22] A. Paszke et al., "Pytorch: An imperative style, high-performance deep learning library," in *Advances in Neural Information Processing Systems 32*, H. Wallach et al., Eds. Curran Associates, Inc., 2019, pp. 8024–8035.
- [23] A. Fan et al., "Training with quantization noise for extreme fixed-point compression," *arXiv preprint arXiv:2004.07320*, 2020.
- [24] B. Jacob et al., "Quantization and training of neural networks for efficient integer-arithmetic-only inference," in *IEEE Conference on Computer Vision and Pattern Recognition*, 2018.